

Tuning and Improvements in a Waypoint and Trajectory Tracking Algorithm

Peter Bauer*

Assistant Research Fellow, Budapest, H-1111 Hungary

József Bokor†

Scientific Director, Budapest, H-1111 Hungary

This paper deals with waypoint guidance and trajectory tracking of aircrafts. After briefly introducing a previously published and a newly developed waypoint guidance strategy (publishing real flight test results also), it makes a literature review. The goals of the work are set based on this review. Considering these goals, the fine tuning of the newly developed algorithm is done first. Then linear and circular waypoint reachability maneuvers are examined. It is pointed out that it is better to start to turn away from the waypoint if it is unreachable then turn toward it if it becomes reachable. Finally, the article extends the capabilities of the new algorithm to track given parametric spatial trajectories. This extended capability is demonstrated in a simulation example.

I. Introduction

Aircraft waypoint guidance and trajectory tracking is an actual and important topic especially for UAVs which should complete missions in limited space. Here, waypoint guidance means catching given reference points with a given tolerance, trajectory tracking means flying along a given spatial path curve.

The authors are involved in a project ([1]) where a waypoint guidance law is applied onboard a small UAV. This guidance law is described in detail in [2]. During the simulation and flight tests a few disadvantages of this method were discovered.

A new waypoint guidance method was proposed in [3] and compared with the original (in [2]) method including real flight test results.

The goal of this work is to make a more extensive literature review mapping the possible alternative waypoint guidance and trajectory tracking solutions. The proposed method (in [3]) can be reviewed, improved and tuned based on the literature.

The organization of the rest of the paper is as follows: Section II briefly describes the strategy proposed in [2] and points out its disadvantages presenting simulation results. Section III shortly describes the proposed new strategy summarizing its properties. Section IV makes the literature review collecting the possible necessary properties of a waypoint guidance or trajectory tracking solution. The author's solution is reviewed based on this list and the possible necessary improvements are listed. Finally the further aims of this paper are enumerated. Section V describes the tuning of controller parameters obtaining the optimal values. Section VI compares linear and circular reachability maneuvers from the view of required path lengths. Section VII demonstrates the capability of the solution to track a given spatial parametric trajectory. Finally section VIII concludes the paper.

*Assistant Research Fellow, Computer and Automation Research Institute, Hungarian Academy of Sciences, Kende u. 13-17. Budapest, Hungary H-1111

†Scientific Director, Computer and Automation Research Institute, Hungarian Academy of Sciences, Kende u. 13-17. Budapest, Hungary H-1111

Copyright © 2012 by the American Institute of Aeronautics and Astronautics, Inc. The U.S. Government has a royalty-free license to exercise all rights under the copyright claimed herein for Governmental purposes. All other rights are reserved by the copyright owner.

The above statements are visualized using software-in-the-loop (SIL) simulation results. The SIL for Ultrastick UAV (see [1] and [4]) was used.

Three test cases were run (the waypoint positions are given in meters relative to the starting point using East (E) and North (N) notations) with $k = 1$ tuning value and without wind effects.

1. To track a path with far waypoints:
 $0E/0N, -100E/-100N, -2100E/-100N$
2. To track a path with close waypoints:
 $0E/0N, -100E/-100N, -300E/-100N$
3. To track a path with very close waypoints:
 $0E/0N, -100E/-100N, -170E/-100N$

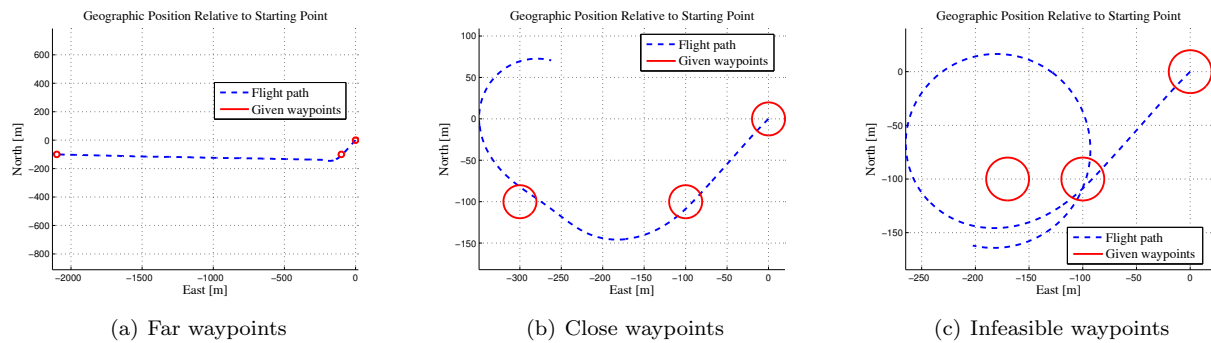


Figure 2. Waypoint tracking case study.

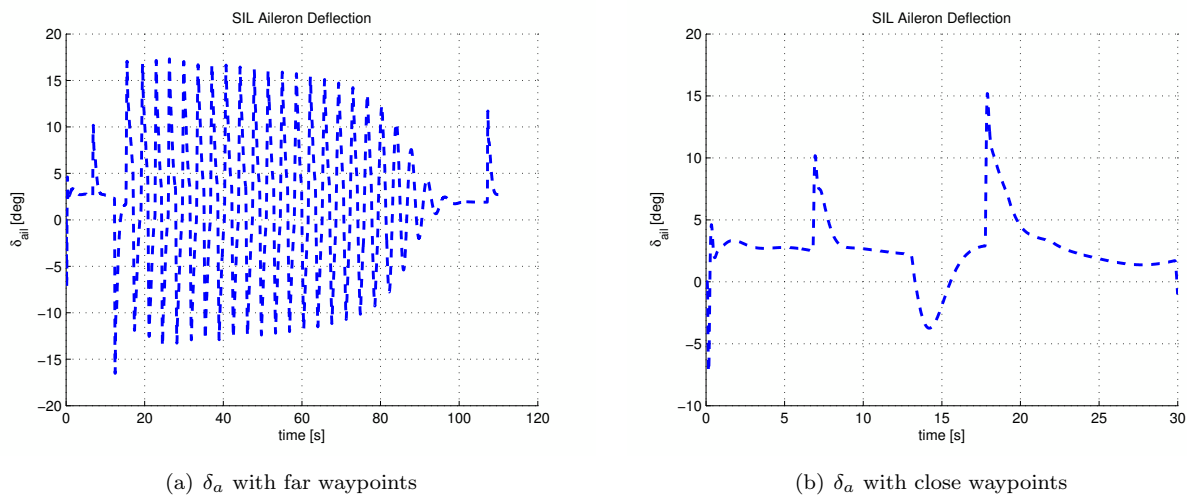


Figure 3. Aileron deflections in waypoint tracking case study.

The results can be seen in figures 2 and 3. The circles denote the given waypoints with the 20m tolerance radius.

Figure 2(a) and (b) show that the aircraft tracks both the far and close waypoints well. But it is worth to see the aileron deflections in figure 3. In the first case almost bang-bang control is applied while the aircraft is far from the waypoint. This is not an acceptable behavior and proves the first and second statements. Figure 2 (c) shows the limit cycle when the waypoint is unreachable with the given aircraft.

These disadvantages should be corrected by developing a new waypoint guidance strategy. This new strategy is introduced in the next section (III).

III. A new waypoint guidance strategy

The goal in the development of this strategy was to overcome the difficulties of the other strategy introduced in the previous section. This algorithm is based on azimuth angle difference between azimuth angle of aircraft velocity vector and azimuth angle between aircraft position and waypoint (called as track azimuth angle ψ^T and defined in Eq. 3). All azimuth angles are defined relative to the North axis of Earth coordinate system (coord. sys.). This provides proper scaling according to the situation. If the waypoint is far, small azimuth angle difference results from the same lateral miss distance (see figure 4).

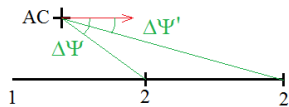


Figure 4. Azimuth angle differences for far and close waypoints

Figure 4 shows that the azimuth angle difference becomes smaller if the next waypoint is farther from the aircraft and this is the required behavior. This way the scaling problem is solved. In the following, the details of the algorithm are described.

In case of reaching a waypoint (or start of tracking control) the algorithm first checks if aircraft flying direction is within a $\pm ATOL^\circ$ range relative to the track azimuth angle ψ^T (see figure 5 where X^E, Y^E is Earth coord. sys.). Here 10 was a sufficiently small $ATOL$ angle value selected by engineering intuition. The optimal $ATOL$ value will be determined in section V.

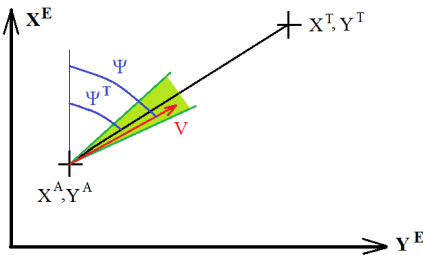


Figure 5. Decision about tracking method with $\pm ATOL^\circ$ range constraint

In figure 5 X^A, Y^A is aircraft current position in Earth coord. sys., X^T, Y^T is the position of the next waypoint. The track azimuth angle can be calculated as:

$$\psi^T = \arctan \left(\frac{Y^T - Y^A}{X^T - X^A} \right) \quad (3)$$

Actual aircraft azimuth angle (ψ) is estimated using the attitude estimation EKF (see [5] [6]).

If ψ is within the $\pm ATOL^\circ$ range relative to ψ^T the aircraft flies directly towards the waypoint. This is called linear path segment tracking. During linear path segment tracking the aircraft calculates the track azimuth angle and the azimuth angle difference in all time steps.

If ψ is out of the $\pm ATOL^\circ$ range relative to ψ^T the aircraft approaches the point using a circular path. This is called circular path segment tracking.

It starts with the calculation of the circular path to be followed and checking of waypoint reachability. At first, the possible turn radius is calculated considering the equation of coordinated turn:

$$R = \frac{V^2}{\tan \phi_0 \cdot g \cdot k} = \frac{(u^E)^2 + (v^E)^2}{\tan \phi_0 \cdot g \cdot k} \quad (4)$$

Here, V is the horizontal velocity of aircraft relative to the ground (calculated from North (u^E) and East (v^E) velocity components in Earth coord. sys. measured with GPS), ϕ_0 is the turn bank angle, g is the gravitational constant and k is a correction factor to make R larger ($0 < k \leq 1$). ϕ_0 is chosen to be constant 25° to make it possible to track the circle within $\pm 40^\circ$ roll angle range (this limitation is applied because non-aerobatic aircrafts are considered only). The best value of k will be obtained in section V.

After calculating the radius of circle, its center point should be calculated according to Eq. 5. Here, $\Delta\psi$ gives the direction of turn (right or left turn). After calculating the circle center, the reachability of the waypoint is checked.

$$\begin{aligned}\Delta\psi &= \text{sign}(\psi^T - \psi) \cdot 90^\circ \\ X^C &= X^A + R \cos(\psi + \Delta\psi) \\ Y^C &= Y^A + R \sin(\psi + \Delta\psi)\end{aligned}\tag{5}$$

The strategy for waypoint catching is to track the circle while aircraft azimuth angle reaches the $\pm ATOL^\circ$ range relative to the waypoint (see figure 6). At this point, the algorithm can change to linear segment tracking and fly directly to the waypoint.

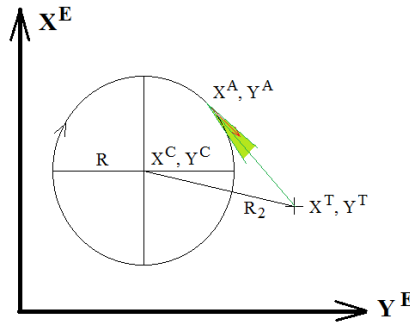


Figure 6. Change from circular segment tracking to linear segment tracking

The existence of this transition point is guaranteed if the waypoint is outside of the circle. So, waypoint reachability can be checked by checking if the waypoint is inside or outside of the circle. This is done considering the distance of the waypoint from the circle center (see figure 6) and a safety distance of TOL m (considering imperfect circle tracking in high wind conditions):

$$\begin{aligned}R_2 &= \sqrt{(X^T - X^C)^2 + (Y^T - Y^C)^2} \\ \text{if } R_2 > R + TOL &\rightarrow \text{reachable} \\ \text{else not reachable}\end{aligned}\tag{6}$$

If the waypoint is reachable, the aircraft starts to track the circle by tracking a virtual waypoint along it. This waypoint is s m arc length forward of the aircraft along the circle. Its position is calculated as follows:

$$\begin{aligned}\psi^C &= \arctan\left(\frac{Y^A - Y^C}{X^A - X^C}\right) \\ \bar{\psi}^C &= \psi^C + \\ &+ \text{sign}((X^A - X^C) \cdot v^E - (Y^A - Y^C) \cdot u^E) \frac{s}{R} \\ X^T &= X^C + R \cdot \cos(\bar{\psi}^C) \\ Y^T &= Y^C + R \cdot \sin(\bar{\psi}^C)\end{aligned}\tag{7}$$

Here, in the second equation the sign of the vector product of the vector pointing from circle center to the aircraft position and aircraft velocity vector is considered, because this gives the flight direction along the circle. s is the arc length (will be tuned in section V) and ψ^C is aircraft's azimuth angle along the circle (azimuth angle of the point on the circle closest to the aircraft).

If the waypoint is unreachable, the algorithm guides the aircraft to fly straight ahead until the waypoint becomes reachable, see figure 7.

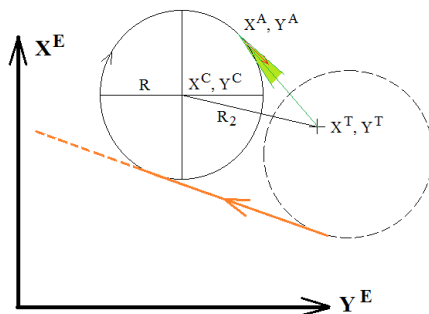


Figure 7. Straight flight until original waypoint (X^T, Y^T) becomes reachable

During this flight, the circle is calculated and reachability is checked in every time step. If the waypoint becomes reachable, the algorithm changes to circular segment tracking. This strategy can prevent flying in a limit cycle if the tolerance in Eq. 6 is large enough, but it is still possible to end in a limit cycle especially in high wind conditions.

Until the waypoint is unreachable, the aircraft tracks a virtual waypoint two circle diameter ahead of the aircraft (this point is fixed when unreachability is detected and remains unchanged until reachability is satisfied):

$$\begin{aligned} X^T &= X^A + 4R \cdot \cos(\psi) \\ Y^T &= Y^A + 4R \cdot \sin(\psi) \end{aligned} \quad (8)$$

This way the strategy has three modes from which two needs the same tracking solution:

1. Flying straight towards the next waypoint (linear path segment tracking).
2. Flying straight towards a virtual waypoint to provide waypoint reachability (linear path segment tracking).
3. Flying along a circle (circular path segment tracking).

Both linear and circular path segment tracking is done with an azimuth angle difference based control of the aircraft. This can be done using a simple proportional controller which converts the azimuth angle difference to a roll angle reference value. This value can be tracked by the aircraft low level controller (see [4] [7]). The proportional control law is as follows:

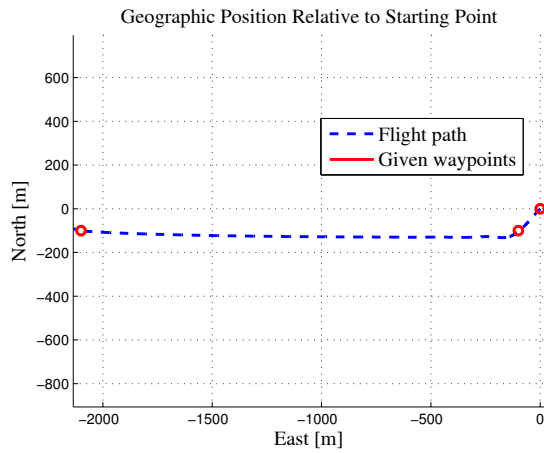
$$\phi_{ref} = \text{sign}(\psi^T - \psi) \cdot \min(k_\phi \cdot |\psi^T - \psi|, 40^\circ) \quad (9)$$

The k_ϕ gain will be tuned in section V.

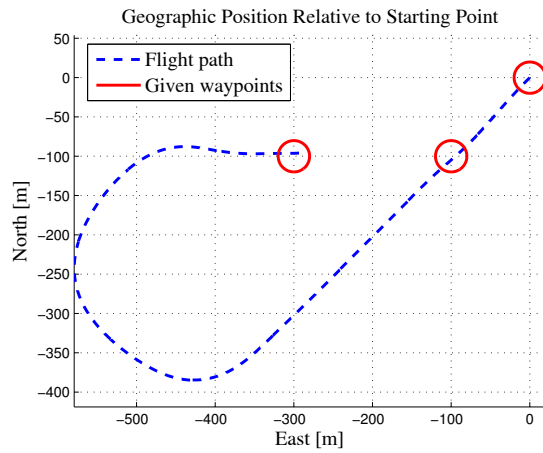
To prove that the drawbacks of the previous method were removed, the same simulations as in the previous section were done with this new method. The results can be seen in figure 8.

Figure 8 (a) does not show large difference compared to figure 2 (a) but there is no oscillation in aileron deflections as figure 8 (d) shows. So, there is a large improvement compared to the other method.

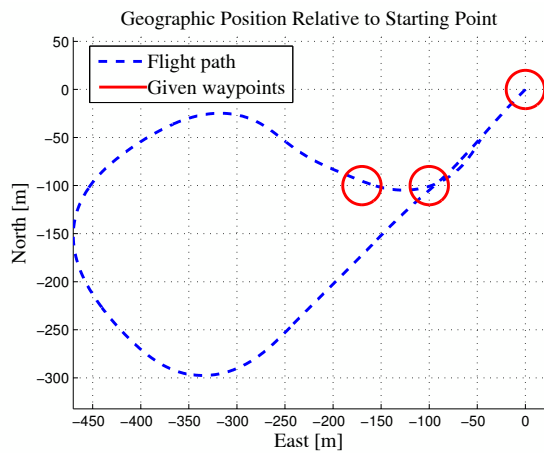
The tracking of close waypoint seems to be worse with the new method (compare figure 8 (b) with figure 2 (b)) because the waypoint was classified as unreachable thanks to the tolerance in reachability decision. But this provides that, the originally unreachable point becomes reachable as figure 8 (c) shows.



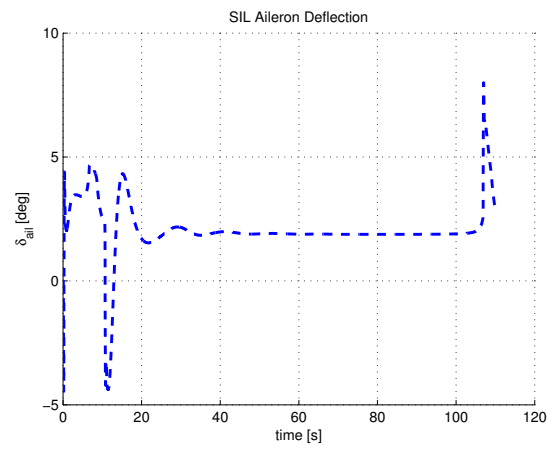
(a) Far waypoints



(b) Close waypoints



(c) Infeasible waypoints



(d) δ_a with far waypoints

Figure 8. Waypoint tracking case study.

The properties of this new strategy are as follows:

1. It makes possible to fly between given fixed waypoints. The flight path between the points is not constrained.
2. It is scaled by the real situation, gentle control for far, aggressive control for close waypoints.
3. It checks and guarantees waypoint reachability.
4. It considers aircraft dynamics calculating turn radius from coordinated turn requirement.
5. It has two modes: the approach stage with circular or linear + circular segment tracking and the final stage with linear segment tracking.
6. It tracks the given path based on azimuth angle difference, using bank angle control of the aircraft.

III.A. Real flight test results

In this subsection the results of two flight tests are presented. The task was to catch given waypoints with the aircraft in all two cases.

In the first case the old waypoint guidance strategy (from [2]) was tested with four waypoints. In the second case, the proposed new strategy with the azimuth angle based guidance law was tested with three waypoints. The results are shown in figure 9.

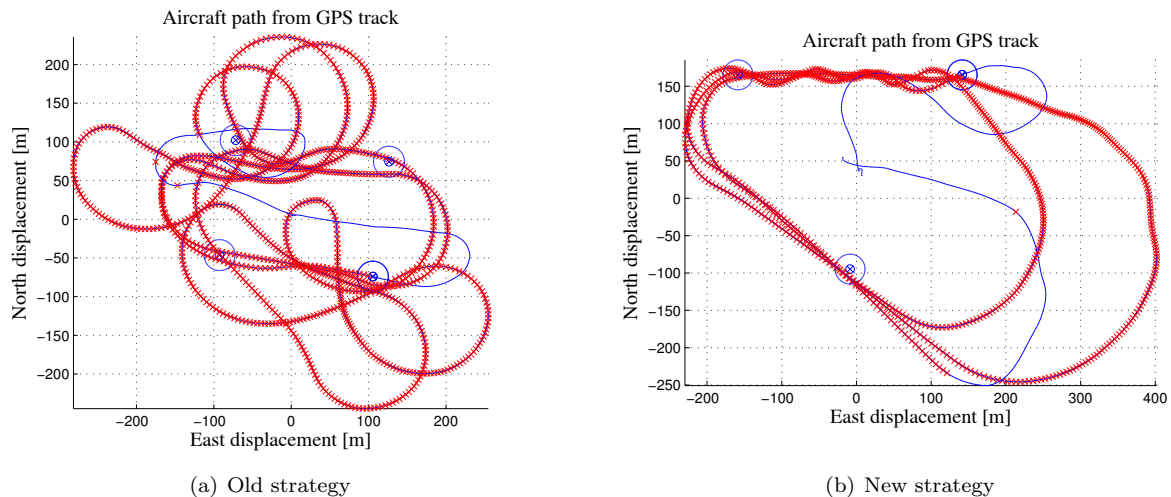


Figure 9. Real flight test results.

The figures show that the old law misses the waypoints several times, that's why it makes 'circles' to catch them. The new law successfully catches all the points and has almost identical paths between the three points except for the last section. This section is affected by the West-East wind which had variable velocity.

This means that the proposed new law outperforms the old one. In the next section an extensive literature review will be done to decide about the possible direction(s) of further development.

IV. Review of waypoint guidance and trajectory tracking literature

[8] deals with the tracking of a given spatial curve. A virtual point is moved along the target trajectory and the goal is to decrease the cross track and the direction error to zero. A nonlinear backstepping strategy is used which assumes the knowledge of vehicle dynamics.

[9] describes a proportional navigation method. The goal is to decrease the line-of-sight rate to zero (to hold the target direction relative to the aircraft constant). This is similar to the linear segment tracking case in the previous section, when the aircraft flies towards a given point. But the point is moving in this article! The problem is solved using nonlinear model predictive control (MPC).

[10] this solution is similar to [8] it tracks a moving virtual point along the given trajectory. A required azimuth angle is approximately calculated based on cross track and lookahead distances.

[11] describes a fuzzy approach based tracking method which is able to catch moving waypoints with a given heading angle. It very well lists the possible goals and problems in waypoint guidance which will be used in listing the possible goals in this article.

In [12] a very similar method to the one described in the previous chapter can be found. It controls the turning rate and heading angle of the aircraft. It has a shortpath and lowturning requirement which means calculating the possible shortest path between two points and turning on a radius as large as possible. It considers waypoint reachability but not flies straight forward in case of unreachable waypoint. It makes a turn in the other direction instead. It considers coordinated turn and error tolerance in trajectory generation. It applies two stage control with turning stage and transitional (final) stage.

[13] This solution is similar to the one published in [9]. It controls the line-of-sight using a Lyapunov function based technique.

Considering all of this literature sources and our achievements (in the previous section) the above possible goals can be listed:

1. To use a more sophisticated control technique such as fuzzy logic, nonlinear MPC, backstepping and Lyapunov function based nonlinear techniques instead of the simple bank angle based proportional control.
2. To provide waypoint reachability with the shortest possible path. This could require a turning maneuver instead of flying straight ahead.
3. To track a given spatial trajectory with the aircraft instead of catching only a few waypoints.
4. To track moving waypoints.
5. To cross fixed or moving waypoints with a given heading and/or velocity.

Considering the above possible goals the goals of this work were decided as follows:

1. Avoid using sophisticated (and so complicated) nonlinear control methods if the simple method is satisfactory. This requires fine tuning of the parameters ($ATOL$, k_ϕ , k , s).
2. To make the shortest possible reachability maneuver. Our method basically flied straight ahead in case of an unreachable point while the point became reachable. A possible alternative solution is proposed in [12] where the aircraft makes a turn in the opposite direction from the given waypoint. This accelerates the increase in the distance between aircraft and point. But does it result in a shorter overall path to the point? This should be tested.
3. To test the proposed method in parametric spatial trajectory tracking.

The above goals give the work of the forthcoming sections.

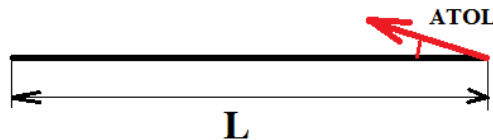


Figure 10. The used notations in linear segment tracking fine tuning

V. Fine tuning of controller parameters

This section deals with the fine tuning of controller parameters described in section III. At first, it makes the fine tuning of linear segment tracking, then it deals with the fine tuning of circular segment tracking. Tuning was done using SIL simulations without wind disturbances.

V.A. Fine tuning of linear segment tracking

The performance of linear segment tracking control can be dependent from *ATOL* heading angle tolerance, k_ϕ controller gain in Eq. 9 and the length of the linear segment. The fine tuning regarding these parameters was done by making a lot of SIL simulations with different parameters. The *ATOL* parameter was considered as the initial direction difference of the aircraft from the line (see figure 10).

Three different path lengths were considered ($L = 50m$, $L = 200m$, $L = 1000m$) with several different k_ϕ and *ATOL* values. The nonlinear aircraft SIL simulation was run and the time averaged absolute tracking error was calculated in all cases. The results are summarized in tables 1, 2, 3 (the first column shows the value of k_ϕ parameters, the first row shows the value of *ATOL* parameters, while the inside shows the time averaged absolute tracking error).

Table 1. Tuning parameters and time averaged absolute errors [m] with L=50m

k_ϕ / ATOL [deg]	0	5	10	15	20	25	30
0.1	0.16	1.17	2.56	4.09	5.84	8.49	194.65
0.25	0.16	1.16	2.53	4.04	5.76	8.06	125.95
0.5	0.17	1.13	2.48	3.88	5.53	7.58	10.86
1	0.18	1.08	2.39	3.74	5.24	7.13	7.97
3	0.23	0.91	2.2	3.66	5.22	7.13	9.79
6	0.29	0.87	2.2	3.66	5.22	7.13	9.79
10	0.32	0.87	2.2	3.66	5.22	7.13	9.79

Table 2. Tuning parameters and time averaged absolute errors [m] with L=200m

k_ϕ / ATOL [deg]	0	5	10	15	20	25	30
0.1	274.1	4.73	4.43	10.86	17.8	360.3	498
0.25	170.46	4.65	3.97	7.89	13.25	18.56	23.79
0.5	7.38	4.43	3.95	5.45	8.3	11.84	15.39
1	4.93	3.7	3.7	4.39	5.51	6.97	9
3	1.79	1.48	1.36	2.04	3.81	6.36	9.22
6	0.85	0.94	1.4	2.16	3.86	6.38	9.31
10	0.86	0.99	1.47	2.2	3.9	6.43	9.33

Table 3. Tuning parameters and time averaged absolute errors [m] with L=1000m

k_ϕ / ATOL [deg]	0	5	10	15	20	25	30
0.1	5159	4179	3273	2508	2034	1888	2042
0.25	2288	1906	1569	1297	1135	1097	1155
0.5	22.8	19.3	16.3	13.94	12.27	11.6	11.87
1	11.53	9.97	8.65	7.56	6.68	6.07	6.11
3	3.87	3.35	2.56	1.93	2.3	3.66	5.73
6	1.91	1.62	1.24	1.1	2.2	4.15	6.51
10	1.89	1.65	1.31	1.23	2.37	4.27	6.6

From the tables it is obvious that small k_ϕ gains give very large errors (except for some cases). That is why plots were constructed considering k_ϕ from 1 to 10 only. The plots can be seen in figures 11.

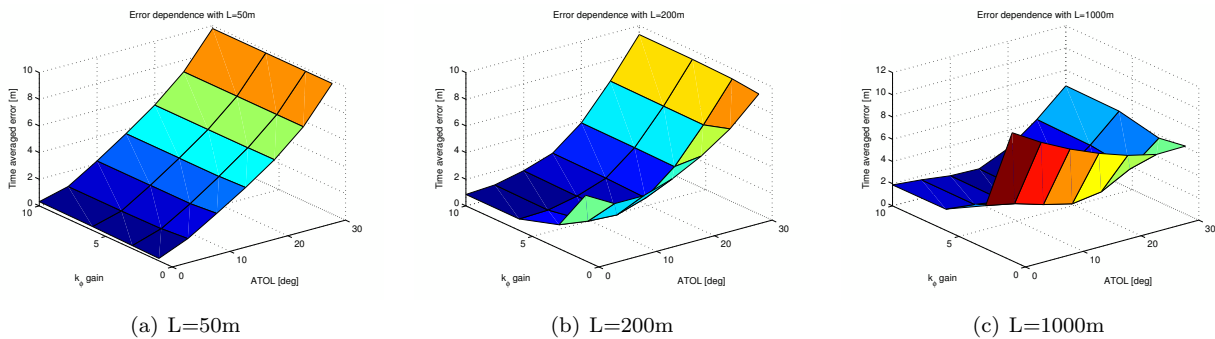


Figure 11. Parameter dependence of time averaged absolute errors in linear segment tracking

From the figures and from calculations it resulted that the optimum k_ϕ should be between 2 and 8 and the optimum $ATOL$ parameter should be between 0 and 10 irrespective of the segment length. Considering this statements another calculation with SIL was run considering the parameter ranges below:

$$k_\phi = [2 \ 3 \ 4 \ 5 \ 6 \ 7 \ 8] \quad ATOL = [0 \ 5 \ 10] \quad L = [25 \ 50 \ 100 \ 200 \ 400]$$

From these calculations similar plots and data were got. The final optimal k_ϕ resulted as 6 and the final optimal $ATOL$ as 10 irrespective of the segment length. This way the optimal parameters for linear segment tracking were determined. The next step is the determination of optimal parameters for circular segment tracking.

V.B. Fine tuning of circular segment tracking

The performance of circular segment tracking control can be dependent from k correction factor, s forward arc length and k_ϕ controller gain. The fine tuning regarding these parameters was done by making a lot of SIL simulations with different parameters considering $V = 20m/s$ ground speed and calculating turn radius according to Eq 4. The flight task was to fly a circle. Four different k values were considered: 1 0.65 0.3 0.1 (1 for smallest possible and 0.1 for 10 times larger circles) with several different k_ϕ and s . The time averaged absolute errors are summarized in tables 4, 5, 6, 7 (the first column shows the value of k_ϕ parameters, the first row shows the value of s parameters, while the inside shows the time averaged absolute tracking error).

The data are plotted in figures 12, 13. Here, k_ϕ values above 1 are good again. The optimum k_ϕ and s values were determined with minimum seeking in Matlab for every k value. The results are shown in table 8. The table shows that the optimum k_ϕ gain is 3 and the optimum s forward arc length is 75m irrespective of the k scaling (the mean value of the achieved optimal s values is 76.25 which is close to 75). Now only the optimal k should be chosen. The average error largely decreases by decreasing k , but this means larger and larger turn radii which makes waypoint tracking more and more complicated and requires more and more time to be tracked. Finally, $k = 0.65$ was selected to avoid extremely large turning radii. Note that the 5.7m average absolute tracking error is well inside the given 20m tolerance radius of waypoints.

Table 4. Tuning parameters and time averaged absolute errors [m] with $k=1$

k_ϕ / s [m]	5	10	40	75	115	200
0.1	218.9	221.8	34.9	34.6	231.3	224
0.25	95.8	102.8	125.5	135	134.8	116.5
0.5	36	32.1	45.6	53.4	51	25.3
1	42.9	38.8	21.7	17.8	9.4	16.7
3	39.9	34.6	14.2	10.9	13.6	19.6
6	39.9	32.8	14.6	11.4	15.5	19.6
10	39.5	32.4	15.2	11.8	16.1	19.6

Table 5. Tuning parameters and time averaged absolute errors [m] with k=0.65

k_ϕ / s [m]	5	10	40	75	115	200
0.1	263.7	20.1	19.6	19.6	19.4	18.8
0.25	57.5	67.5	103.1	124	134	128.3
0.5	34.3	26	35	46	48.4	32.1
1	43	36	12.8	14.8	8.9	21
3	42.9	32	6.6	5.7	18.9	46.38
6	41.2	30.7	7.3	8.7	24	49
10	40.8	30.3	8.3	6.9	22.9	48.7

Table 6. Tuning parameters and time averaged absolute errors [m] with k=0.3

k_ϕ / s [m]	5	10	40	75	115	200
0.1	5.8	6.1	7.6	339.5	367.1	399.1
0.25	21.5	20.7	50	75	93.4	111.5
0.5	34	27.1	18.7	28.1	34.9	32.3
1	43.2	36	7.6	10	8.2	9.1
3	43	37.1	1	2.2	9.8	37.9
6	43.2	37.2	2.86	5.2	14.2	45.3
10	43.3	37.4	3.5	4.2	14	46.4

Table 7. Tuning parameters and time averaged absolute errors [m] with k=0.1

k_ϕ / s [m]	5	10	40	75	115	200
0.1	1.1	1.3	76.7	122.1	165	235.9
0.25	25	19.3	1	1.2	1.3	1.28
0.5	39.8	31.9	8.1	0.85	0.84	0.79
1	47.4	38.7	3.6	5.3	5.8	1.7
3	47.5	40.1	0.65	0.26	2.6	12.8
6	47.5	40.3	2.3	1.5	4.6	16.3
10	47.6	40.4	2.7	1.2	4.5	16.9

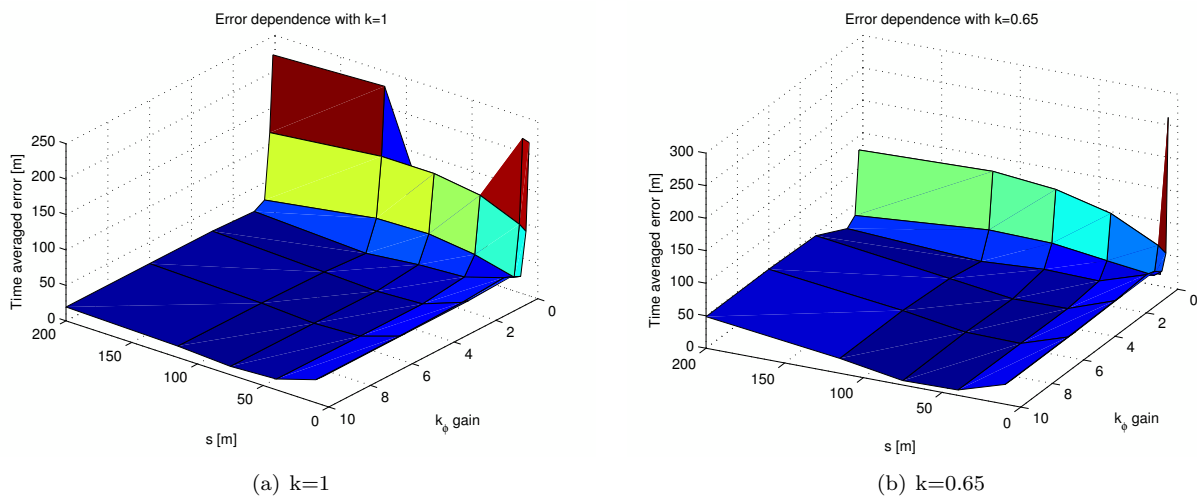


Figure 12. Parameter dependence of time averaged absolute errors in circular segment tracking

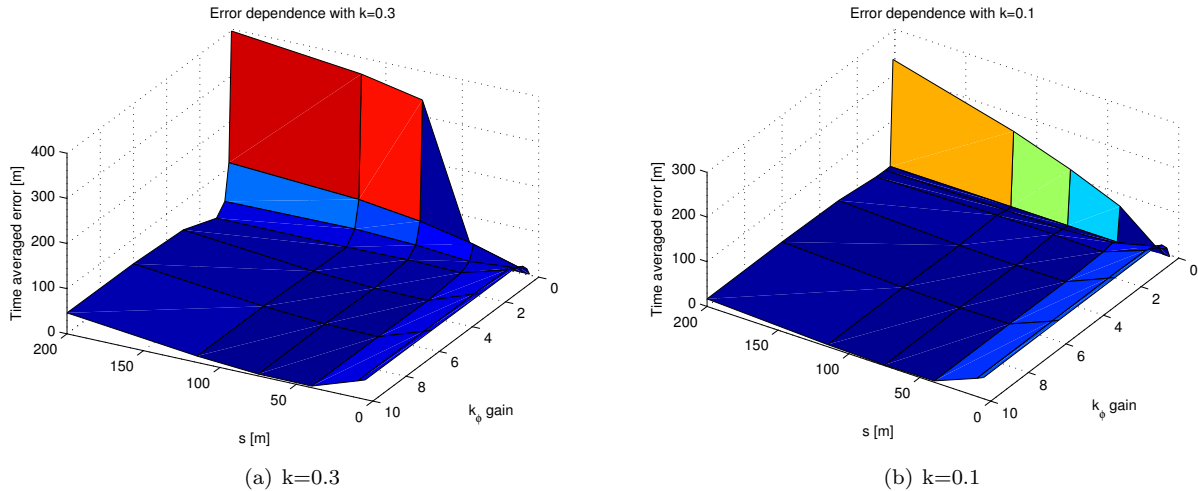


Figure 13. Parameter dependence of time averaged absolute errors in circular segment tracking

Table 8. Optimum parameters from circular segment tracking fine tuning

k	k_ϕ OPT	s OPT [m]	err OPT [m]
1	1	115	9.44
0.65	3	75	5.7
0.3	3	40	1.037
0.1	3	75	0.266

After fine tuning of controller parameters the problem of linear or circular reachability maneuver was considered in the next section.

VI. Linear or circular reachability maneuver? Which is optimal?

In section III waypoint reachability was solved by flying straight ahead until the waypoint becomes reachable (see figure 7). However, [12] suggests to turn away from the waypoint on a circle until the waypoint becomes reachable. The question is that which solution requires less flight time? This can be decided calculating the required flight path lengths and comparing them.

The two different situations are shown in figure 14. In the first case the aircraft flies along a linear path segment until the waypoint X^T, Y^T becomes reachable. Then it follows the circle centered at X^{C2}, Y^{C2} until it reaches the $\pm ATOL^\circ$ range. Finally it flies straight toward the point. In the second case the aircraft turns along the circle centered at X^C, Y^C until the waypoint X^T, Y^T becomes reachable. Then it follows the circle centered at X^{C2}, Y^{C2} until it reaches the $\pm ATOL^\circ$ range. Finally it flies straight toward the point.

It is not trivial which solution results in shorter flight paths, so it was calculated in an example. Several waypoints were generated along a circle considering the tolerance (TOL) also. The generated points for different distances from the tolerance limit are shown in figure 15(a). The figure shows the possible turn circle of the aircraft (inner blue), the tolerance circle (outer blue) and three point sets with different distances from the tolerance circle. The left side is straight because the aircraft was assumed to be in $(0, 0)$ with 90° azimuth angle and all the points should be on the right side of it. The calculated points are parameterized with their azimuth angle relative to the circle center $(0, 150)$.

The required path lengths from the aircraft position to the target point were calculated both with linear and circular reachability maneuvers. The resulting path lengths are shown in figure 15(b). The figure shows that the required path lengths of the linear maneuvers are larger or equal with the path lengths of the circular maneuvers. This means that the circular maneuvers are optimal with smaller required path lengths, so in the future these should be used in the tracking.

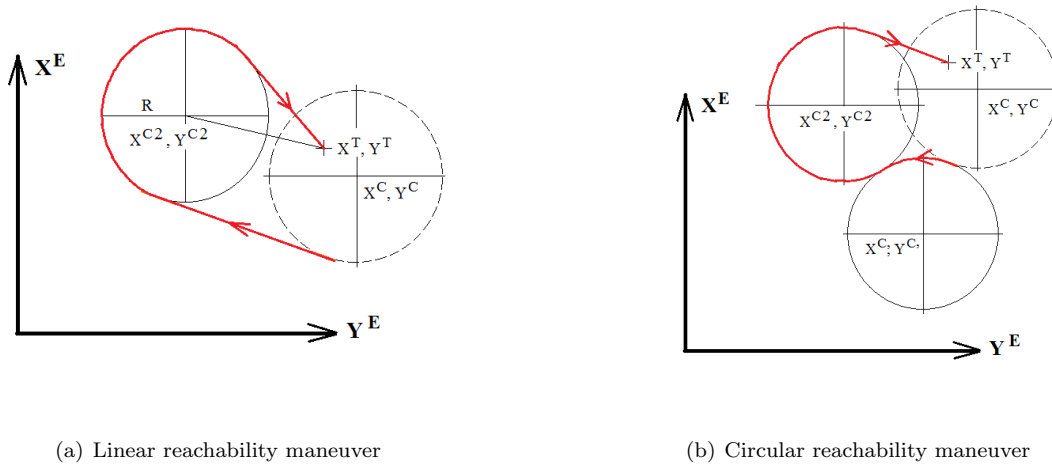


Figure 14. Possible reachability maneuvers

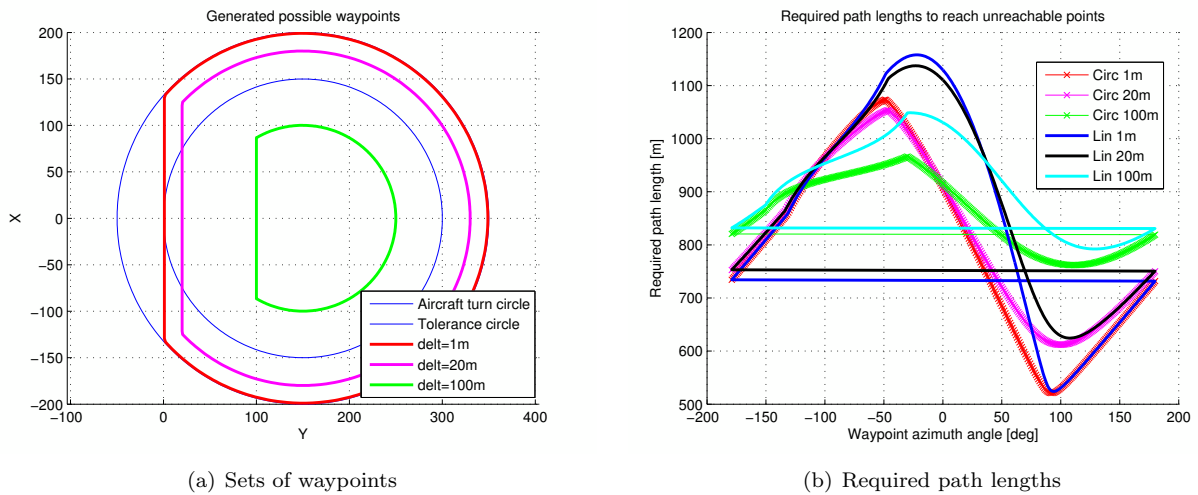


Figure 15. Waypoints and required path lengths

VII. Tracking of a given parametric spatial trajectory

The tracking of circular path segments is done with moving a virtual point along the circle and tracking this point with the aircraft. This is really similar to the case of tracking a parametric spatial curve. So, the latter application possibility is worth to be tested. This is done in this section.

VII.A. Theoretical background

Assume that the trajectory to be tracked is a spatial, parameterized curve (in the XY plane) given by the following functions:

$$\begin{aligned} X &= f_x(p) \\ Y &= f_y(p) \end{aligned} \quad (10)$$

Eq. 10 is parameterized by the parameter p . It is required to have smaller or equal curvature in every p point than the maximum feasible curvature from aircraft dynamics point of view. Now, and later on a simplified trajectory is used as an example, but most of the formulae will be derived for the general case. The example curve is given by:

$$\begin{aligned} X &= p \\ Y &= A \sin\left(\frac{2\pi}{T}p - \frac{\pi}{2}\right) + A = f(X) \end{aligned} \quad (11)$$

Where A is the amplitude, T is the period distance and $\frac{\pi}{2}$ is the offset. The curvature of such a curve can be calculated as follows:

$$C = \frac{|\ddot{f}(X)|}{(1 + \dot{f}(X)^2)^{3/2}} = \frac{1}{R} \quad (12)$$

In Eq. 12 $\dot{f}(X)$ means $\frac{df(X)}{dX}$. The turn radius in each point can be calculated as:

$$R = \frac{(1 + \dot{f}(X)^2)^{3/2}}{|\ddot{f}(X)|} = \frac{\left(1 + A^2 \frac{4\pi^2}{T^2} \left(\cos\left(\frac{2\pi}{T}p - \frac{\pi}{2}\right)\right)^2\right)^{3/2}}{\left|-A \frac{4\pi^2}{T^2} \sin\left(\frac{2\pi}{T}p - \frac{\pi}{2}\right)\right|} \quad (13)$$

The minimum and maximum radii are as follows:

$$\begin{aligned} X = \frac{T}{2} \quad R &= \frac{T^2}{A4\pi^2} \\ X = \frac{3T}{4} \quad R &= \infty \end{aligned} \quad (14)$$

Eq. 14 shows that if one knows the minimum possible turn radius of the aircraft the trajectory can be tuned to be feasible selecting appropriate A and T values. The expressions also show that a sinusoidal curve is a very good test curve because it has a continuously varying radius from ∞ to a given minimum. This means that a continuously varying curvature should be tracked by the aircraft.

After defining the trajectory it can be tracked by moving a virtual point along it in a given lookahead distance (s) forward of the aircraft. Assume that aircraft starting position and the initial parameter value for the first virtual point (p_0) along the curve are known. Then the aircraft moves towards the point and the point position should be generated in every time step. This can be done by calculating the orthogonal projection of aircraft position to the parametric curve and the position of virtual point from this projected point considering the given lookahead distance. Finally the p parameter giving the position of the virtual point should be obtained. But the steps of this two step calculation are extremely difficult for parametric curves.

A simplified solution can be obtained by determining the intersection of an aircraft position centered circle with radius s and the parametric curve:

$$\begin{aligned} X^A + s \cos(\psi_A) &= f_x(p) \\ Y^A + s \sin(\psi_A) &= f_y(p) \end{aligned} \quad (15)$$

Here, the two unknowns are ψ_A and p , but closed form solution is also extremely difficult for parametric curves described by highly nonlinear $f_x(p)$ and $f_y(p)$ functions.

The problem can be approximately solved by the following multi step calculation:

1. Calculate the estimated position of the virtual point (X^V, Y^V) considering aircraft velocity.
2. From this estimated position calculate the possible p and ψ_A parameter values.
3. Finally, refine the results with Newton-Raphson iteration.

Step 1:

The estimated next virtual point position can be calculated considering the tangent vector of the curve in the previous position (always denoted by p_0), aircraft ground velocity (V) and time step of solution (Δt) (because the virtual point should move together with the aircraft):

$$\begin{aligned} X^V &= f_x(p_0) + \frac{\dot{f}_x(p_0)}{\sqrt{\dot{f}_x(p_0)^2 + \dot{f}_y(p_0)^2}} V \Delta t \\ Y^V &= f_y(p_0) + \frac{\dot{f}_y(p_0)}{\sqrt{\dot{f}_x(p_0)^2 + \dot{f}_y(p_0)^2}} V \Delta t \end{aligned} \quad (16)$$

Step 2:

Because the estimated point (X^V, Y^V) is not exactly on the curve two different p values can be calculated from the X^V and Y^V positions. Their average can be the approximate p parameter value.

$$\begin{aligned} p_x &= f_x^{-1}(X^V) \\ p_y &= f_y^{-1}(Y^V) \\ p &= \frac{p_x + p_y}{2} \end{aligned} \quad (17)$$

The possible ψ_A can be calculated as follows:

$$\psi_A = \text{atan2} \left(\frac{f_y(p) - Y^A}{f_x(p) - X^A} \right)$$

Step 3:

The nonlinear expression to be made to zero is (derived from Eq. 15):

$$\Phi(z) = \begin{bmatrix} X^A + s \cos(\psi_A) - f_x(p) \\ Y^A + s \sin(\psi_A) - f_y(p) \end{bmatrix} = 0 \quad z = \begin{bmatrix} \psi_A \\ p \end{bmatrix} \quad (18)$$

The Newton-Raphson iteration for this expression is:

$$\begin{aligned} &\text{given } z_0 \\ \Delta z &= - \left[\frac{\partial \Phi(z)}{\partial z} \Big|_{z_0} \right]^{-1} \Phi(z_0) \\ z_0 &= z_0 + \Delta z \\ &\text{repeat until } \Delta z < \text{tolerance} \end{aligned} \quad (19)$$

In our case the inverse function can be calculated in closed form:

$$\frac{\partial \Phi(z)}{\partial z} = \begin{bmatrix} -s \sin(\psi_A) & -\dot{f}_x(p) \\ s \cos(\psi_A) & -\dot{f}_y(p) \end{bmatrix} \quad (20)$$

$$\left[\frac{\partial \Phi(z)}{\partial z} \right]^{-1} = \begin{bmatrix} -\dot{f}_y(p) & \dot{f}_x(p) \\ -s \cos(\psi_A) & -s \sin(\psi_A) \end{bmatrix} \frac{1}{s \sin(\psi_A) \dot{f}_y(p) + s \cos(\psi_A) \dot{f}_x(p)}$$

The inverse exists if $s \sin(\psi_A) \dot{f}_y(p) + s \cos(\psi_A) \dot{f}_x(p) \neq 0$. This expression is the scalar product of the vector pointing from aircraft position to the curve and the curve tangent vector. The product is zero if the two vectors are perpendicular. This is the case when p gives the orthogonal projection of aircraft position to the curve. In this case p should be left unchanged, otherwise the iteration can be done.

Because UAVs have limited computational capacity, the iteration is stopped by the number of steps (3 steps are done) instead of a given tolerance for Δz . After developing this trajectory tracking solution it was tested in SIL simulation.

VII.B. SIL flight test

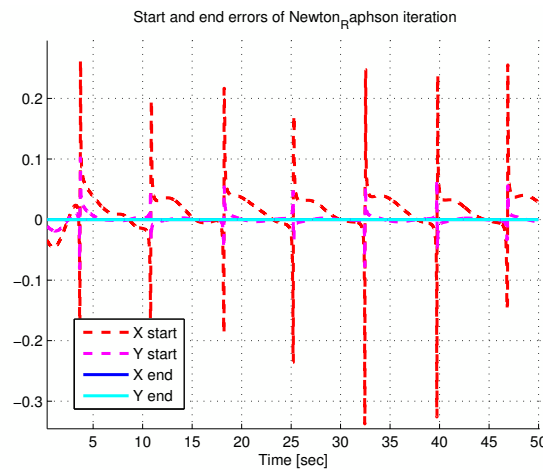


Figure 16. Starting and end error terms of Newton-Raphson iteration

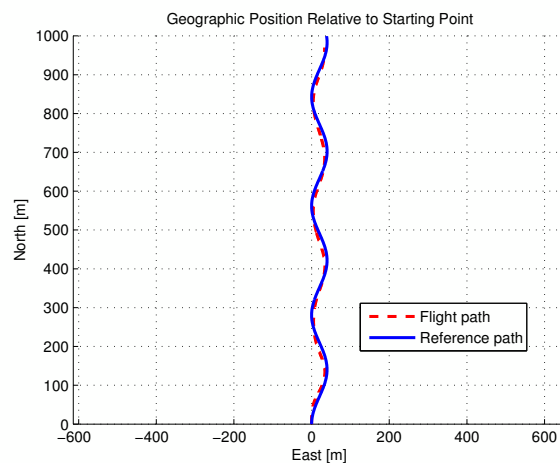


Figure 17. The tracking of a given spatial trajectory

The parameters of the sinusoidal reference trajectory were chosen as $A = 20$, $R = 100$, $T \approx 281$. T was calculated from Eq. 14. The parameters of the controller were the optimal ones selected in section V ($s = 75$, $k_\phi = 3$). The circular tracking gain was used because of continuously varying curvature.

Results are shown in figures 16, 17. The first figure shows that the 3 step Newton-Raphson iteration is very effective, it decreases the error of the solution to very close to zero. The second figure shows that the aircraft tracks the sinusoidal trajectory very well.

SIL simulations with other parameter values were also done, but the detailed evaluation was left to the future.

VIII. Conclusion

This paper first described a waypoint guidance strategy from [2] and pointed out its disadvantages. Then repeated the derivation of a new solution which corrects these disadvantages (published originally in [3]). Simulation and real flight test results prove the efficiency of the new method. This inspired the authors to further develop it. This development starts with extensive literature review. From the literature the possible further development steps were determined and some of them was implemented here. The first step was the fine tuning of the algorithm to achieve the possible best results. The second step was the examination of linear or circular reachability maneuvers from path length point of view. It was pointed out that the circular maneuvers result in shorter paths and so, they are better. The final step was the development of the strategy to track a prescribed reference trajectory. This trajectory can be given by a parameterized spatial curve. The contribution of this article is to relatively simply (and accurately) calculate the position of the virtual point to be tracked. This section ends with a simulation example which shows the success of the method.

Considering the literature review part, the further developments can be:

1. Real flight tests of the circular reachability maneuvers and the trajectory tracking.
2. Development to be able to cross waypoints with a given heading.
3. Development to track moving waypoints (target points).

Acknowledgments

The authors gratefully acknowledge the support of the EU project ' ACTUATION 2015: Modular Electro Mechanical Actuators for ACARE 2020 Aircraft and Helicopters ' under grant agreement no: 284915. This work is supported by the Office of Naval Research Global, Grant Number N62909-10-1-7081, Dr. Paul Losiewicz program officer. This work is also supported by the Control Engineering Research Group of HAS at Budapest University of Technology and Economic.

References

- ¹Paw, Y. C., "UAV Research Group," 2006.
- ²Niculescu, M., "Lateral Track Control Law for Aerosonde UAV," *Proc. of the 39th AIAA Aerospace Sciences Meeting and Exhibit*, AIAA, Reno, NV, USA, January 2001.
- ³Bauer, P., "Comparison of Aircraft Waypoint Guidance and Tracking Strategies," *In Proc. of 9th European Workshop on Advanced Control and Diagnosis (ACD 2011)*, Budapest, Hungary, November 2011.
- ⁴Paw, Y. C., *Synthesis and Validation of Flight Control for UAV*, Ph.D. thesis, University of Minnesota, 2009.
- ⁵Bauer, P. and Bokor, J., "Development and Hardware-in-the-Loop Testing of an Extended Kalman Filter for Attitude Estimation," *Proc. of 11th IEEE International Symposium on Computational Intelligence and Informatics*, Budapest, Hungary, 2010, pp. 57–62.
- ⁶Bauer, P. and Bokor, J., "Multi-Mode Extended Kalman Filter for Aircraft Attitude Estimation," *Proc. of IFAC World Congress 2011*, IFAC, Milano, Italy, August 2011.
- ⁷Bauer, P. and Bokor, J., "Infinite horizon LQ optimal output tracking from development to real flight tests," *In Proc. of 12th IEEE International Symposium on Computational Intelligence and Informatics (CINTI 2011)*, Budapest, Hungary, November 2011, pp. 277–282.
- ⁸Lapierre, L., Soetanto, D., and Pascoal, A., "Nonlinear Path Following Control of Autonomous Underwater Vehicles," *In Proc. of IFAC Workshop on Guidance and Control of Underwater Vehicles*, IFAC, Newport, South Wales, April 2003.
- ⁹Talole, S. E., Ghosh, A., and Phadke, S. B., "Proportional navigation guidance using predictive and time delay control," *Control Engineering Practice*, Vol. 14, 2006, pp. 1445–1453.
- ¹⁰Oh, S.-R. and Sun, J., "Path following of underactuated marine surface vessels using line-of-sight based model predictive control," *Ocean Engineering*, Vol. 37, 2010, pp. 289–295.
- ¹¹Innocenti, M., Pollini, L., and Turra, D., "A Fuzzy Approach to the Guidance of Unmanned Air Vehicles Tracking Moving Targets," *IEEE Transactions on Control Systems Technology*, Vol. 16, No. 6, November 2008, pp. 1125–1137.

¹²Zhu, R., Sun, D., and Zhou, Z., "Integrated design of trajectory planning control for micro air vehicles," *Mechatronics*, Vol. 17, 2007, pp. 245–253.

¹³Guo, J., "A waypoint-tracking controller for a biomimetic autonomous underwater vehicle," *Ocean Engineering*, Vol. 33, 2006, pp. 2369–2380.